3.3 DIFFUSION OF MAGNESIUM AND MICROSTRUCTURES IN Mg^+ IMPLANTED SILICON CARBIDE— W. Jiang, D. J. Edwards, H J. Jung, Z. Wang, Z. Zhu, T. J. Roosendaal, S. Hu, C. H. Henager, Jr., R. J. Kurtz (Pacific Northwest National Laboratory), and Y. Wang (Los Alamos National Laboratory)

OBJECTIVE

Magnesium is predicted as one of the major metallic transmutation products in silicon carbide under high-energy neutron irradiation. As a candidate material for fusion reactor designs, SiC is investigated in this experimental study to obtain data and gain a basic understanding of defect microstructures and Mg diffusion in Mg^+ ion implanted SiC.

SUMMARY

Following our previous reports [1-3], further isochronal annealing (2 hrs.) of the monocrystalline 6H-SiC and polycrystalline CVD 3C-SiC was performed at 1573 and 1673 K in Ar environment. SIMS data indicate that observable Mg diffusion in 6H-SiC starts and a more rapid diffusion in CVD 3C-SiC occurs at 1573 K. The implanted Mg atoms tend to diffuse deeper into the undamaged CVD 3C-SiC. The microstructure with Mg inclusions in the as-implanted SiC has been initially examined using high-resolution STEM. The presence of Mg in the TEM specimen has been confirmed based on EDS mapping. Additional monocrystalline 3C-SiC samples have been implanted at 673 K to ion fluence 3 times higher than the previous one. RBS/C analysis has been performed before and after thermal annealing at 1573 K for 12 hrs. Isothermal annealing at 1573 K is being carried out and Mg depth profiles being measured. Microstructures in both the as-implanted and annealed samples are also being examined using STEM.

PROGRESS AND STATUS

Introduction

Silicon carbide composites (SiC/SiC) have been proposed for structural materials [4] and flow channel inserts [5] in fusion reactor designs. Upon exposure to high-energy neutrons, SiC undergoes nuclear transmutations accompanied with generation of atomic displacements. Sawan et al. [6] has predicted that at a fast neutron dose of ~100 dpa (displacements per atom), there will be ~0.5 at.% Mg generated in SiC among other major transmutation products that include 0.15 at.% Al, 0.2 at.% Be, 0.01 at.% P, 2.2 at.% He and 0.84 at.% H. The impacts on structural stability and property degradation from the displacement damage and the presence of the transmutation impurities in SiC are currently unknown. They need to be investigated and fully evaluated prior to an informed decision for SiC to be utilized in fusion reactors. High-energy neutron irradiation in a prototypical fusion environment would be ideal for investigating the response of SiC microstructures. However, a fusion relevant neutron source capable of generating a meaningful amount of Mg and other elements in SiC for study through transmutation reactions is currently not available. This experimental study uses ion implantation to introduce Mg into the SiC microstructure; post-implantation thermal annealing is applied to recover implantation damage in the structure. Reported here are some of the initial data on Mg diffusion, microstructures with Mg inclusions, and defect accumulation and recovery in Mg^+ ion implanted SiC. Further on-going study of isothermal annealing at 1573 K will lead to determination of the Mg diffusion coefficient in SiC. Microstructural features with Mg inclusions will also be examined. The data may provide a useful basis for modeling and simulation to further understand the physical and chemical processes of Mg interaction with SiC.

Experimental Procedure

The previous monocrystalline (0001)-oriented 6H-SiC and polycrystalline CVD 3C-SiC implanted at 773 K with 200 keV Mg^+ ions to 2.5×10^{16} and 3.2×10^{16} ions/cm^2, respectively, have been further annealed isochronally (2 hrs.) at higher temperatures up to 1673 K. The Mg depth profiles in the SiC samples were measured after each annealing step using time-of-flight secondary ion mass spectrometry (ToF-SIMS)

with 2 keV O_2^+ ions as the sputtering beam and 25 keV Bi^+ ions as the analyzing beam. The depth scale for monocrystalline 6H-SiC with a smooth surface was calibrated by measuring the crater depth with a Veeco Dektak 150 stylus profilometer, while that for polycrystalline CVD 3C-SiC samples is determined based on the same sputtering rate in units of nm/(nA·sec) from 6H-SiC. The microstructure in the implanted depth region of epitaxial (001)-oriented 3C-SiC film (~2 µm thick) on Si has been examined using an FEI aberration-corrected Titan 80-300 scanning electron transmission microscope (STEM). Energy dispersive spectroscopy (EDS) for Mg in the sample has also been conducted using a new JEOL JEM-ARM200CF aberration-corrected STEM with greatly enhanced analytical capability.

In addition, two (001)-oriented 3C-SiC films on Si were implanted 7° off normal with 200 keV Mg^+ ions to an ion fluence of 9.6×10^{16} ions/cm^2 at 673 K. Unlike the previous implantation at 773 K, surface exfoliation of the 3C-SiC films did not occur at the lower temperature (673 K). The ion fluence corresponds to ~6 at. % Mg at the peak maximum according to a SRIM simulation [7]. Although the relative ion fluences are expected to be reasonably accurate, the absolute values could be subject to a large error bar. The implanted sample was cleaved to smaller pieces for different thermal treatments. One piece was annealed at 1373 K for 2 h and the other at 1573 for 12 h to study defect recovery and Mg behavior. The furnace anneals were performed in flowing Ar gas with the sample placed in a chimney of Zr metal foils to minimize or prevent surface oxidation of the SiC sample. For the sample annealed at 1573 K, the center region was covered with flakes of Zr oxide, which was removed prior to making measurements. Two edges of the sample formed unintentional, irremovable layers of Zr oxide. SIMS measurements for Mg profiles in both the center and edge areas were conducted. In addition, the ion-channeling method based on 2.0 MeV He^+ Rutherford backscattering spectrometry (RBS/C) was used to analyze the lattice disorder on the Si sublattice in the center area. The edge area was too small to be probed with RBS/C. The annealed SiC at 1573 K and the as-implanted sample are currently being examined under TEM. Isothermal annealing at 1573 K for times ranging up to 12 h is currently being conducted and ToF-SIMS is being followed to measure the Mg depth profile after each anneal.

Results and Discussion

The normalized SIMS depth profiles of the implanted Mg in 6H-SiC and CVD 3C-SiC annealed at 1573 and 1673 K, together with some of the previous data for lower temperatures are shown in Figure 1. Based on the ion fluences, the peak maxima for the Mg profiles in 6H-SiC and CVD 3C-SiC correspond to ~1.6 at.% and ~2.0 at.% Mg, respectively. The Mg profile in the as-implanted 6H-SiC in Figure 1(a) is located at 255 nm with a full width half maximum (FWHM) of 103 nm. Annealing at higher temperatures up to 1473 K does not lead to a significant change in the peak width [1]; further isochronal annealing at 1573 and 1673 K for 2 h each results in an observable Mg diffusion, as shown in Figure 1, which is somewhat similar to Ag behavior in 6H-SiC [8]. The Mg diffusion is still insignificant with an increase in the peak width (FWHM) from 104 nm at 1473 K to 125 nm at 1673. The Mg profile in 6H-SiC remains somewhat Gaussian up to 1673 K. Compared to its monocrystalline 6H-SiC counterpart, the Mg peak width in as-implanted polycrystalline CVD 3C-SiC below 1473 K is systematically larger by 20-30%, as shown in Figure 1(b). This behavior could be attributed to diffusion enhancing impurities or porosity at the grain boundaries. Similar interpretations have been proposed for Ag diffusion in CVD-SiC [911]. The data in Figure 1(b) suggest that there might be some modest Mg diffusion starting at 1473 K [1]. More rapid Mg diffusion occurs with an increase in the width from 147 nm at 1473 K to 317 nm at 1673 K. Furthermore, the Mg atoms tend to diffuse deeper into the polycrystalline host, making its depth profile highly skewed towards the bulk. The half width of the Mg profile at the greater depth is 136 nm (vs. 102 nm for the other half towards the surface) in CVD 3C-SiC at 1573 K, and 192 nm (vs. 125 nm) at 1673 K. This preferred Mg diffusion into the undamaged crystal is not yet fully understood, but could be associated with implantation induced effects near the surface region. Similar behavior was observed for Ag in CVD-SiC [12]. It should be noted that shifts in peak positions in both 6H-SiC and CVD 3C-SiC are observed and all the peaks except for that in CVD 3C-SiC at 1673 K are repositioned to 255 nm. The peak shifts could originate from various contributors, including SiC surface oxidation [observed for CVD 3C-SiC at 1573 and 1673 K (data not shown)], deposition and redistribution of Zr oxide on SiC surface, and possible sublimation or etching of ion-implanted SiC at high temperatures [13,14]. We are currently performing vacuum anneals to investigate the associated issues.

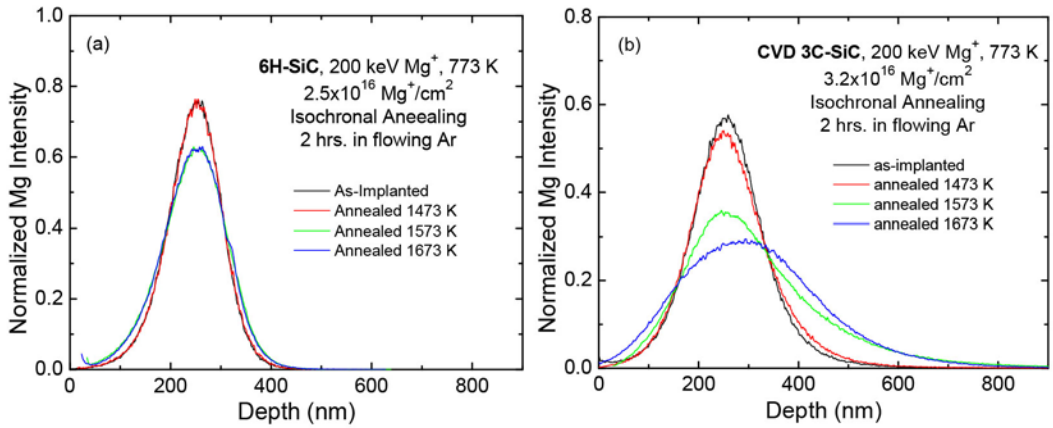

Figure 1. ToF-SIMS depth profiles of Mg in (a) monocrystalline 6H-SiC and (b) polycrystalline CVD 3C-SiC implanted with Mg^+ ions at 773 K and annealed isochronally (2 hrs.) up to 1673 K in Ar environment.

Figure 2 shows two high-angle annular dark field (HAADF) STEM images with different magnifications for 3C-SiC implanted with 200 keV Mg^+ to 3.2×10^{16} ions/cm^2 at 773 K. The lowerresolution image in Figure 2(a) shows a buried implantation band located at depths between 170 and 330 nm. The atomic-level resolution image shown in Figure 2(b) was taken in the depth region near the Mg profile maximum (~255 nm). Some image contrast on the 3C-SiC (110) plane is observed. In-situ EDS analysis has ruled out the possibility of major surface contamination from Ga during the focused ion-beam (FIB) process for TEM specimen preparation. However, either EDS or EELS in the Titan 80-300 STEM system has not detected Mg at 300 keV. The Mg atomic concentration is expected to be ~2 at.% in the depth region from SRIM simulation for an ion fluence of 3.2×10^{16} ions/cm^2, but we cannot exclude the possibility of a large error in the absolute value of the ion fluence at this time. The image contrast is not yet fully understood, but could originate from a number of factors, including Mg aggregation or replacement, presence of vacancies in the darker atomic columns, a change in the local atomic density, and possible electron diffraction due to a part of coherent electron beam under the high-angle geometry. Implantation to a higher ion fluence is needed for a better understanding. An additional implantation (by tripling the ion fluence) and subsequent thermal treatments have been performed. Preliminary characterizations have also been conducted (see below).

In order to confirm the retention of Mg in the TEM specimen, further EDS analysis at 200 keV was performed using an enhanced EDS system in a new JEOL JEM-ARM200CF STEM. The system has an improved sensitivity due to a larger solid angle of an x-ray detector that has a larger area and is located closer to the specimen than a conventional one. The microscope provides a high-intensity electron beam to facilitate EDS analysis as well as microscopy. The EDS spectra from the implanted depth region clearly show a well-resolved Mg Kα line (data not shown). EDS mapping for the TEM specimen was carried out with the data shown in Figure 3. By integrating counts, the Mg depth profile has been obtained and is plotted in Figure 3. This profile is consistent with that determined by SIMS for the as-implanted sample (Figure 1). The result indicates that Mg redistribution in the implanted SiC is insignificant during the FIB process.

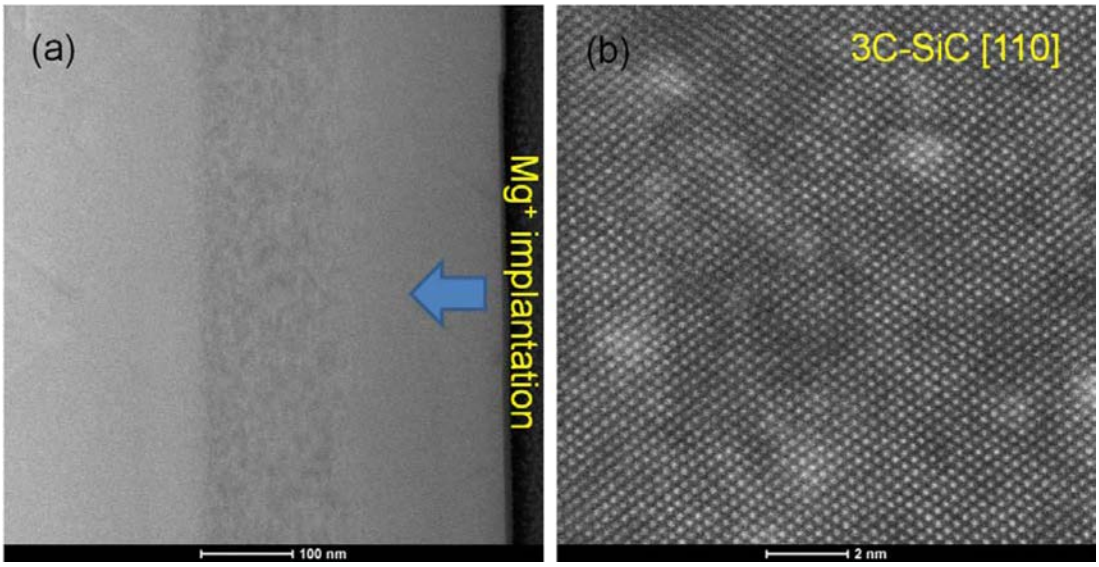

Figure 2. (a) Low-resolution and (b) atomic-level resolution HAADF STEM images for 3C-SiC implanted with 200 keV Mg^+ to 3.2×10^{16} ions/cm^2 at 773 K.

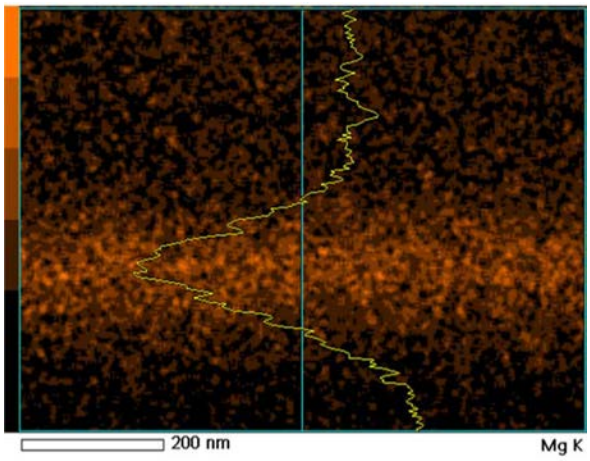

Figure 3. EDS map and depth profile of Mg in 3C-SiC implanted to 3.2×10^{16} Mg^+/cm^2 at 773 K.

Figure 4 shows RBS/C spectra for 3C-SiC implanted to 9.6×10^{16} Mg^+/cm^2 at 673 K, 2 h post-implantation annealed at 1373 K, and 12 h at 1573 K. Channeling and random spectra from an unirradiated area are also included in the figure. It is apparent that the intensity of the damage peak decreases after annealing at 1373 K, indicating that the thermal annealing leads to observable defect recovery. In contrast, the Mg depth profile from SIMS does not change (data not shown), which is consistent with the results for the lower ion fluence reported previously [1]. Further annealing at 1573 for 12 h leads to a nearly complete recovery of the implantation damage. Although the overall dechanneling yield is still slightly higher than that from the unimplanted sample, the damage peak in the annealed sample disappears and the surface peak is comparatively small, suggesting that the surface lattice displacements are also well discovered. It should be noted that in this depth region, the Mg concentration is an order of magnitude smaller than in the as-implanted sample, as shown in Figure 5. The sample surface was covered with Zr oxide flakes after the thermal annealing, which were removed prior to the RBS/C analysis. Possible Mg diffusion to and subsequent release from the surface, SiC sublimation [13,14], or both during the thermal annealing process might be responsible for the low Mg concentration. Unexpectedly, some edge areas were

covered with irremovable Zr oxide layers, where Mg was still retained in SiC without a significant loss. This unintentional layer of Zr oxide may serve as a diffusion barrier to minimize Mg loss. Diffusion of Zr into SiC occurred during the thermal annealing (data not shown), which could affect the Mg migration path in the disordered SiC. The results could be of scientific interest and technological impact, but this is not the focus of the current study. The edge area is being used for STEM study, in addition to the as-implanted sample. A sequence of isothermal annealing at 1573 K up to 720 min, followed by SIMS measurement of Mg depth profile in SiC after each anneal, is also being performed to determine Mg diffusion coefficient in SiC. The data, together with the TEM results will be reported elsewhere at a later time.

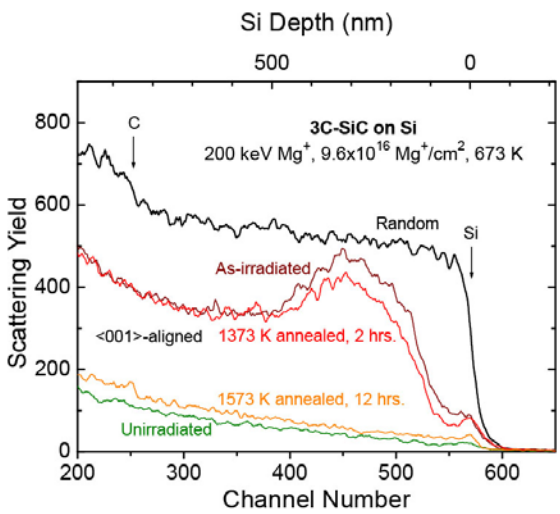

Figure 4. 2.0 MeV He^+ RBS/C spectra along the <001> axis in 3C-SiC implanted with 200 keV Mg^+ ions to 9.6×10^{16} ions/cm^2 at 673 K and post-annealed at higher temperatures. Also included are random and channeling spectra from an unirradiated area.

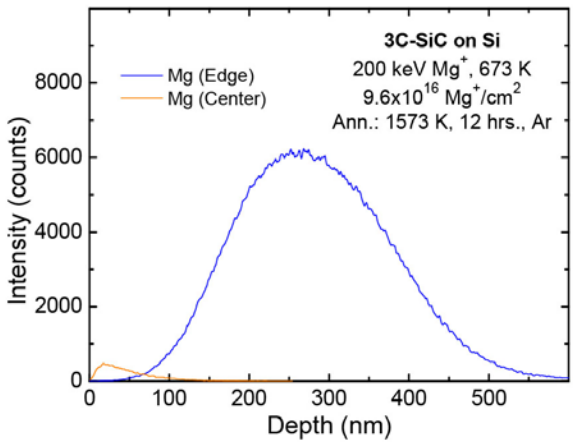

Figure 5. ToF-SIMS depth profiles of Mg in 3C-SiC implanted to 9.6×10^{16} Mg^+/cm^2 at 673 K and annealed at 1573 K for 12 hrs. The center area had flakes of Zr oxide that were removed prior to analysis, while the edge area had an irremovable Zr oxide layer (depth scale corrected).

Acknowledgments

This research was supported by Office of Fusion Energy Sciences, U.S. Department of Energy (DOE) under Contract DE-AC05-76RL01830. A portion of the research was performed using EMSL, a national

scientific user facility sponsored by the DOE's Office of Biological and Environmental Research and located at PNNL. Jiang likes to thank Robert Colby for his early TEM effort and Alicia Certain for her early FIB work. Ion implantation was conducted at Ion Beam Materials Laboratory through a partial support from Center for Integrated Nanotechnologies in Los Alamos National Laboratory.

REFERENCES

[1] W. Jiang, Z. Zhu, T. Varga, M. E. Bowden, S. Manandhar, T. Roosendaal, S. Y. Hu, C. H. Henager, Jr., R. J. Kurtz, and Y. Wang, Fusion Materials Semiannual Progress Report for Period Ending June 30, 2013, DOE/ER-0313/54, U. S. Department of Energy, 70.
[2] S. Y. Hu, W. Setyawan, R. M. Van Ginhoven, W. Jiang, C. H. Henager, Jr., and R. J. Kurtz, J. Nucl. Mater. 448 (2014) 121.
[3] S. Y. Hu, W. Setyawan, W. Jiang, C. H. Henager, Jr., and R. J. Kurtz, Fusion Materials Semiannual Progress Report for Period Ending December 31, 2013, DOE/ER-0313/55, U. S. Department of Energy, 149.
[4] A. R. Raffray, R. Jones, G Aiello, M. Billone, L. Giancarli, H. Golfier, A. Hasegawa, Y. Katoh, A. Kohyama, S. Nishio, B. Riccardi, and M. S. Tillack, Fusion Eng. Des. 55 (2001) 55.
[5] C. P. C. Wong, M. Abdou, M. Dagher, Y. Katoh, R. J. Kurtz, S. Malang, E. P. Marriott, B. J. Merrill, K. Messadek, N. B. Morley, M. E. Sawan, S. Sharafat, S. Smolentsev, D. K. Sze, S. Willms, A. Ying, and M. Z. Youssef, Fusion Eng. Des. 85 (2010) 1129.
[6] M. E. Sawan, Y. Katoh, and L. L. Snead, J. Nucl. Mater., 442 (2013) S370.
[7] J. F. Ziegler, J. P. Biearsack, and U. Littmark, The stopping and Range of Ions in Solids (Pergamon Press, New York, 1985); available from: http://www.SRIM.org.
[8] W. Jiang, W. J. Weber, V. Shutthanandan, L. Li, and S. Thevuthasan, Nucl. Instrum. Method Phys. Res. B 129-220 (2004) 642.
[9] E. Friedland, T. Hlatshwayo, and N. van der Berg, Phys. Status Solidi C 10 (2013) 208.
[10] E. J. Olivier and J. H. Neethling, J. Nucl. Mater., 432 (2013) 252.
[11] E. López-Honorato, H. Zhang, D. Yang, and P. Xiao, J. Am. Ceram. Soc. 94 (2011) 3064.
[12] E. Friedland, J. B. Malherbe, N. G. van der Berg, T. Hlatshwayo, A. J. Botha, E. Wendler, and W. Wesch, J. Nucl. Mater., 389 (2009) 326.
[13] M. A. Capano, S. Ryu, J. A. Cooper Jr., M. R. Melloch, K. Rottner, S. Karlsson, J. Elec. Mater., 28 (1999) 214.
[14] T. T. Hlatshwayo, J. B. Malherbe, N. G. van der Berg, A. J. Botha, and P. Chakraborty, Nucl. Instrum. Method Phys. Res. B 273 (2012) 61.